Supporting Info

Graphene for Controlled and Accelerated Osteogenic Differentiation of Human Mesenchymal Stem Cells

Tapas R. Nayak,[†,▽] Henrik Andersen,[‡,▽] Venkata S. Makam,[†] Clement Khaw,[§] Sukang Bae,[⊥] Xiangfan Xu,[‡] Pui-Lai R. Ee,[†] Jong-Hyun Ahn,[⊥,∥] Byung Hee Hong,[⊥,¶] Giorgia Pastorin,[†,#,▲,] and Barbaros Özyilmaz[‡,#,▲,*]*

Substrates

Figure S1 shows AFM images of graphene on Si/SiO_2. The graphene surface topography consists of flat areas (<1nm RMS) separated by ~8 nm high ripples, which are caused by the difference in thermal expansion of the Cu foil (on which graphene is grown) and the graphene sheet itself (Li *et al., Science*, **2009**, *324*, 1312).

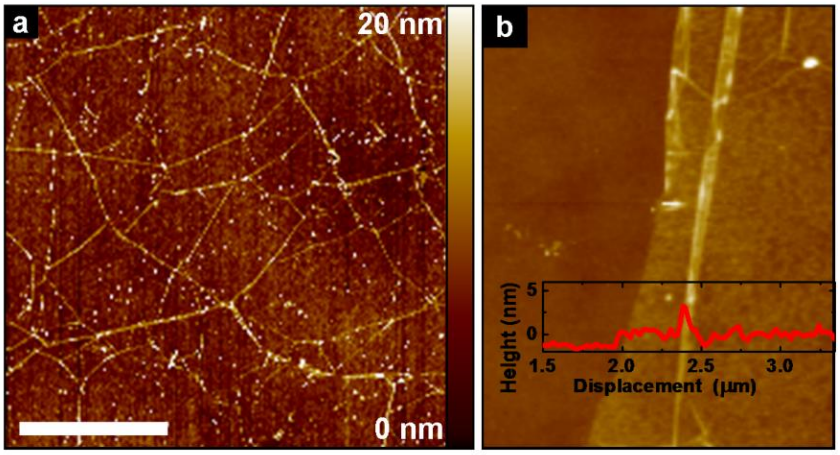

Figure S1. (a) Large scale AFM image of graphene coated Si/SiO_2. The graphene surface shows small ripples and few protrusions but is uniformly only one atom thick. Scale bar is 10μm. (b) AFM image of a partially graphene covered Si/SiO_2 substrate. A step like increase in thickness of ~1nm is due to the presence of graphene.

The surface roughness and Young's modulus of the various substrates used for these studies are summarized in Table S1.

Substrate	R_a (nm)	R_q (nm)	R_z (nm)	E (MPa) (typical literature values)
Si/SiO_2	0.21	0.27	4.27	$70x10^3$
PET	0.47	0.66	7.66	$1\text{-}15x10^3$
PDMS	0.49	0.66	6.52	0.2-1
PDMS with graphene	0.63	0.87	14.3	3
CVD Graphene on Si/SiO_2 (Bi-layer)	0.41	0.78	7.56	$1x10^6$
Carbon coated glass slide	0.79	1.28	13.4	$70x10^3$
Glass slide	1.01	1.46	11.9	$70x10^3$

Table S1. Substrates overview. Roughness was measured by AFM and evaluated by three parameters: Average deviation from mean (R_a), Root Mean Square deviation (R_q) and the peak-to-peak distance (R_z). Young's Modulus E corresponds to typical literature values.

Cell viability study

Four graphene-coated Si/SiO_2 chips, four uncoated Si/SiO_2 chips and eight cover slips (four as negative control and four as positive control) were placed in 24 well plates. Trypan blue assay was used to count the number of viable hMSCs. By using the information obtained from the trypan blue assay, hMSCs were seeded at a density of 20000 cells/ml into the above mentioned wells and incubated for 3 days in a humidified jacketed incubator (Binder), with a temperature of 37°C, 5% CO_2. On 2nd day 50µl of 1% sodium dodecyl sulphate (SDS) was added to positive control wells to induce cell death and continued with incubation.

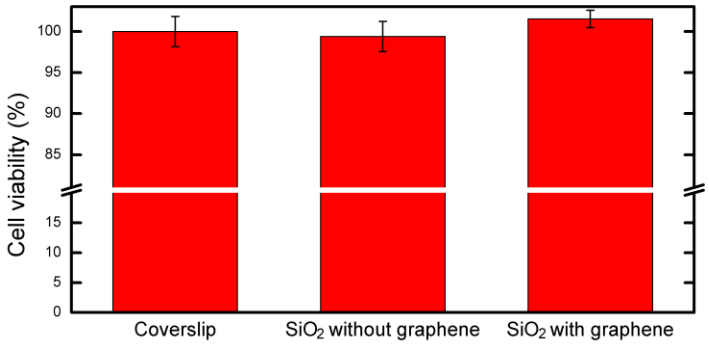

Figure S2. Graph showing the percentage of cell viability of hMSCs after 24 hours exposure to graphene-coated SiO_2 chips (right) in comparison to hMSCs grown on cover slips (left) and uncoated SiO_2 chips (center) as determined by MTT assay.

Assessment of cell viability was also determined using metabolic activity assays, 3-(4, 5-dimethylthiazol-2-yl)-2, 5-diphenyltetrazolium bromide (MTT) (Duchefa Biochemie). In this case, the test principle is based on the reduction of the tetrazolium salt from yellow color to purple color by the mitochondria present in viable cells (Mosmann, *J. Immun. Met.* **1983**, *65*, 55). After 3 days the 24 well plate was taken out from the incubator and all samples with growing cells were transferred to wells of another 24 well plate. 500 µl of tetrazolium salt (0.1 mg/ml) were added to each well including wells having no cells as blank and allowed to incubate for 4 hours in the jacketed incubator. After 4 hours, the contents in each well were pipetted out and 500 µl of DMSO were added to lyse the cells and to solubilize the insoluble formazan dye.

The plate was shaken for 3 minutes to ensure homogeneity of color and aid solubilization of the dye prior to measure absorbance. The absorbance was recorded using the Benchmark plus Micro plate Spectrophotometer (Bio-Rad Laboratories) at 590 nm. The absorbance recorded is directly proportional to the number of viable cells present. All the experiments were repeated in triplicates and the results were expressed as the mean value. The cell viability was calculated in the following way:

$$\text{Cell viability} = \frac{\text{Absorbance of test - Absorbance of blank (PBS)}}{\text{Absorbance of control - Absorbance of blank (PBS)}}$$

Student t-test was used to calculate p-value. If the p-value was found to be less than the threshold (0.05) chosen for statistical significance, then the null hypothesis (which states that the two groups do not differ) was rejected in favor of an alternative hypothesis, which states that the groups do differ significantly. As seen from Figure S2, there was no significant difference ($p>0.05$) in the percentage of cell viability of hMSCs growing on graphene-coated SiO_2 chips in comparison to hMSCs growing on uncoated SiO_2 substrates and cover slips. This result suggests that graphene is non-cytotoxic. The percentage of cell viability data as found from the above MTT assay was comparable to the percentage of cell viability as determined by cell viability by image analysis (as shown in the main text Figure 2a).

Experiment on flow cytometry

The evaluation by fluorescence-activated cell sorting (FACS) further supports the reported data by providing a quantitative evaluation of cell populations presenting specific characteristics. This represents, in our case, the ability of hMSCs to differentiate into osteogenic lineage once adequately stimulated. The hMSCs grown on different substrates (i.e. cover slips, uncoated Si/SiO_2 and graphene-coated Si/SiO_2) were subjected to differentiation with osteogenic medium

(in the presence or absence of BMP-2) and analyzed after 14 days by FACS. The harvested cells were fixed with 4% paraformaldehyde by incubating for 20 minutes. After centrifugation at 1500 RPM for 5 minutes and washing with PBS, the cell pellets were suspended in 100 mM glycine for 10 minutes to quench. The cells were then again centrifuged, washed with PBS, and permeabilized by incubating in 50 µl of 0.1% Triton X for 30 minutes. Subsequently, the cells were washed with PBS and incubated with mouse antihuman osteocalcin antibody for 30 minutes at room temperature. The cells were further washed with PBS and incubated with FITC conjugated goat anti mouse IgG for another 30 minutes. Finally, the cells were washed 2-3 times with PBS and were analyzed using BD LSR II flow cytometer (Becton Dickinson).

The obtained results are summarized in the FACS histogram in Figure S3 and confirm the results obtained with alizarin red quantification (see main text Figure 4). Figure S3 displays a single measurement parameter (relative fluorescence intensity due to FITC) on the x-axis and the number of events (cell count) on the y-axis. While the osteocalcin positive cell population, representing osteogenically differentiated hMSCs, can be found in form of single distinct shifts beyond relative fluorescence intensity of 10^3, the undifferentiated hMSCs can be found in form of single histogram below such value.

As expected, negligible osteocalcin positive cells were found in case of hMSCs on substrates incubated in normal medium (histogram a). The expression of osteocalcin was maximal for all the substrates in osteogenic media with both graphene and BMP-2. This is similar to the results obtained with the alizarin red quantification and confirms the synergistic effect when both graphene and BMP-2 are concurrently present. Interestingly, osteogenic medium with graphene,

in absence of BMP-2, reached almost the same levels of cell differentiation (83%) as those in osteogenic medium with both graphene and BMP-2 (100%). Taken together, both Alizarin Red Quantification and FACS analysis provide a quantitative proof on the ability of graphene to accelerate stem cell differentiation even in the absence of additional growth factor.

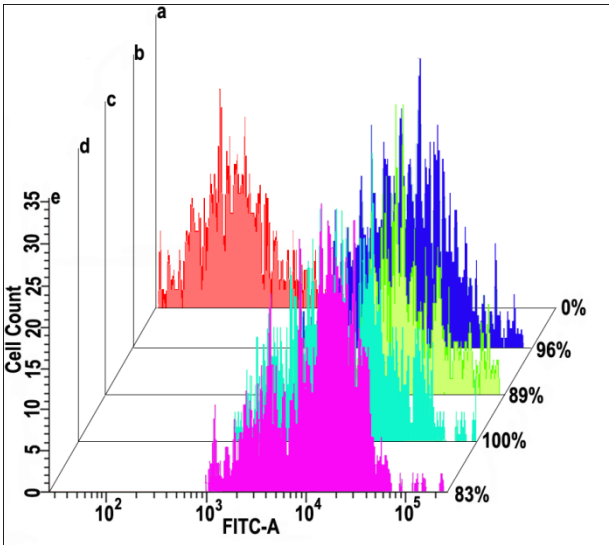

Figure S3: FACS analysis after 14 days of incubation of hMSCs. Curve a (red): Cover slips without osteogenic media (OM) and without BMP-2 (negative control, 0% of differentiation); Curve b (dark blue): Cover slips with both OM and BMP-2 (96% of cell differentiation); Curve c (green): Si/SiO_2 with both OM and BMP-2 (89% of cell differentiation); Curve d (light blue): Graphene with both OM and BMP-2 (synergistic effect, 100% of cell differentiation); Curve e (magenta): Graphene with only OM, without BMP-2 (83% of cell differentiation).

Control experiments with amorphous carbon

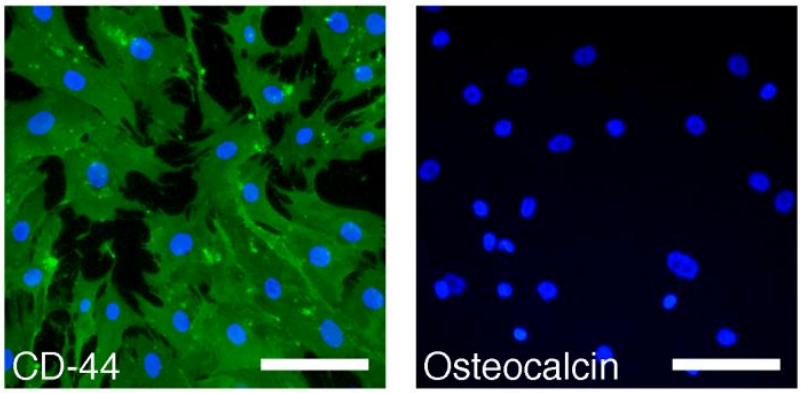

Figure S4. Immunostaining of cells growing on amorphous carbon-coated substrates. CD-44 (left) was still fully visible, while osteocalcin (right) was not visible. Scale bars are 100µm.

The osteogenic effect could in principle also take place in the presence of continuous thin carbon films. To verify the significance of graphene, substrates were coated with a thin layer of carbon using a JEE-420 vacuum evaporator. The thickness of the carbon coating was determined by AFM to be approximately 10 nm. These samples were then subjected to immunostainng of CD-44 and osteocalcin, similar to previous experiments. The carbon coated samples did not show a decrease in CD-44-fluorescence (Figure S4 left), indicating no sign of differentiation. Equally important, no osteocalcin was stained (Figure S4 right), confirming that no cell differentiation towards osteoblasts occured. Thus, a thin layer of carbon is insufficient to render stem cells osteogenic.

Additional material parameters potentially responsible for accelerated stem cell differentiation in graphene coated substrates.

a) Influence of surface chemistry

The role of defects and surface functionalization in CNTs has been heavily studied, but still remains not fully elucidated. The situation may in fact be more complex and may in part be also due to an increase in wettability of the CNT surfaces after plasma treatment. An increase of hydrophilicity is well correlated with an improved adhesion of hMSCs onto the substrates (Baik *et al.*, *Small*, **2011**, *7*, 741; Martins *et al.*, *Small*, **2009**, *5*, 1195).

Pristine graphene is known to be hydrophobic, however we see no degradation in adhesion compared to samples without graphene and observe an increase in differentiation instead. On the other hand, the chemicals and solvents involved in the preparation of graphene coated substrates could create either functionalized groups physisorbed on the graphene surface or change the hydrophobicity. Furthermore, water molecules and hydroxyl radicals trapped between graphene and substrate during the coating process can also affect the surface energy. The situation becomes even more complex, once we introduce the various media for cell culturing.

b) Influence of surface polarization

Bodhak *et al.* (*Acta Biomaterialia*, **2009**, *5*, 2178) observed that polarized hydroxyapatite substrates have lower contact angle and better wettability. Negatively polarized substrates immersed in simulated body fluid showed enhanced bone like apatite formation compared to unpoled substrates, while positively poled substrates determined direct inhibition of apatite layer. Similarly, human fetal osteoblasts reported good adhesion and proliferation on negatively poled substrates where the positively poled substrate inhibited cell growth. Graphene is generally

observed to be positively charged due to environmental doping. However, the doping level of graphene is on the level of +0.2 μC/cm^2 and hence, much smaller than the doping levels at which a negative result was observed (+4.3 μC/cm^2). This may explain why we do not see any issues with cell growth or adhesion on graphene. This hypothesis could be checked in future experiments by, e.g. depositing graphene on ferroelectric PVDF films of different polarization corresponding to a range of charge density ranging from -3 μC/cm^2 to +3 μC/cm^2 .

c) Influence of thermal conductivity

Thermal properties of graphene could in principle play a role in stem cell differentiation. However, the absence of differentiation on higly oriented pyrolytic graphite (HOPG) demonstrates that this property can only provide a minor contribution. While graphene does have the highest thermal conductivity among the carbon allotropes, what really matters is the thermal conductance, which is orders of magnitude higher in graphite. The thermal conductance of bulk graphite is much higher than what the surface can provide.

d) Influence of electrical conductivity

It has been shown that the electrical conductivity of CNTs does promote nerve cells' growth (Hu *et al. Nano Lett.*, **2004**, *4*, 507; Hu *et al. J. Phys. Chem. B*, **2005**, *109*, 4285; Malarkey *et al. Nano Lett.* **2009**, *9*, 264). Based on these results, it has been speculated that higher electrical conductivity could also lead to better differentiation (Voge *et al. J. Neural Eng.* **2011**, *8*, 011001; Chao *et al. Biochem. Biophys. Res. Commun.*, **2009**, *384*, 426). However, to the best of our knowledge so far no experimental evidence has been provided showing that electrical conductivity itself can lead to accelerated stem cell differentiation. This would also be consistent

with our observation that HOPG does not lead to bone cell differentiation. Here it is important to note, that while the electrical conductivity of graphene exceeds the electrical conductivity of graphite, what really matters is the electrical conductance. Similar to the thermal conductance, also here the electrical conductance of bulk graphite is higher than that of graphene.

Graphene quality after cell removal

It is important to know whether the graphene sheet remains intact during the cell differentiation process over 14 days. In Figure S5 we show a series of Raman spectra and corresponding optical images addressing this question. Figure S5b shows the Raman spectra of graphene on Si/SiO_2 after cell removal. The residual material provides a strong background signal. Super imposed on this are small but discernable Raman peaks. As a reference, we show a sample without graphene, which underwent the same process. The corresponding small Raman specific peaks are clearly absent. We can almost fully remove the background after leaving the samples (shown in Figure S5a) for 24 h in Acetone. The Raman spectra of the resulting sample clearly show the G and 2D peaks, which represent the Raman "fingerprints of graphene". Note also, that the absence of the D-peak at 1350 cm^{-1} indicates the lack of defects to the graphene crystal lattice (Ferrari *et al.* *PRL*, **2006**, *97*, 187401). The optical images also clearly shows that the graphene sheet remains largely intact.

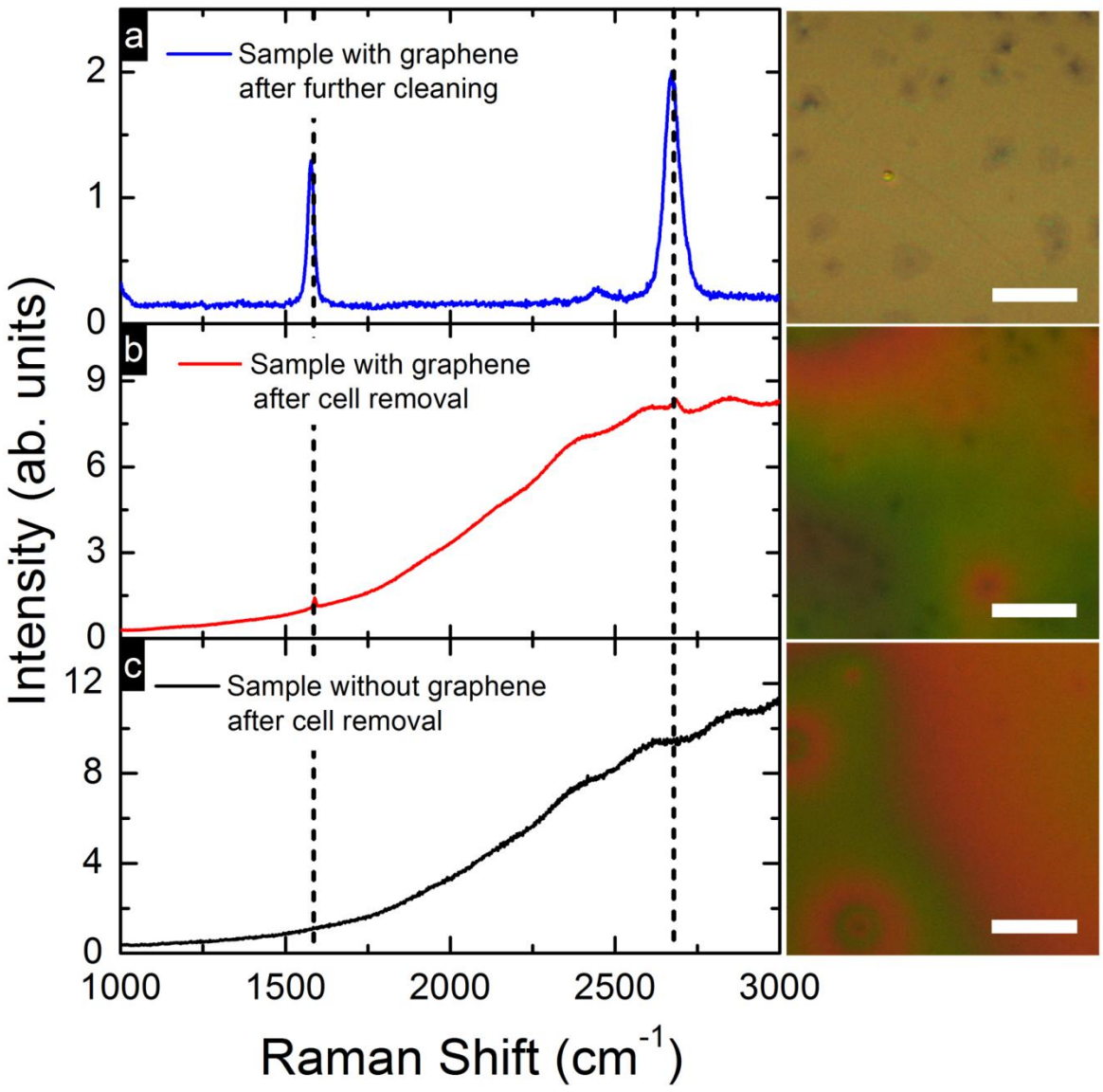

Figure S5: Raman spectrum and optical images of (a) graphene on Si/SiO_2 after removal of cells and cleaning with acetone, (b) graphene on Si/SiO_2 after removal of cells and (c) Si/SiO_2 after removal of cells. Scale bars are 10µm.